



Preparation and Characterization of Nanohybrids Made of Graphene Oxide as Super Adsorbents

KOMAL GROVER¹ and KIRAN JEET^{2*}

¹Department of Mathematics, Statistics, and Physics, Punjab Agricultural University, Ludhiana, Punjab, India.

²Electron Microscopy & Nanoscience Laboratory, Punjab Agricultural University, Ludhiana, Punjab, India.

Abstract

Adsorption is considered one of the best methods for the removal of heavy metal ions from an aqueous solution. However, the synthesis of adsorbents with desired selectivity and performance remains a key challenge in the battle of water decontamination. Recently, carbon-based and metal-oxide based nanomaterials have emerged as promising candidates for the adsorption of heavy metals due to their high specific surface area, high aspect ratio, and concentrated pore size distribution. Here, in this work five adsorbents i.e. Graphene Oxide (GO), Magnetic Graphene Oxide (MGO), Titanium Dioxide (TiO₂), and their composites GO-TiO₂ and MGO-TiO₂ were synthesized. The prepared samples were characterized via high-resolution imaging, BET-N₂ adsorption-desorption analysis, and spectroscopic techniques. TEM results revealed the nanoscale structures of the synthesized nanomaterials. The approximate sizes of MGO and TiO₂ nanoparticles found under TEM studies were about 24.58 and 35.51 nm respectively. The presence of desired functional groups was very well deciphered by FT-IR spectroscopy. Results of N₂ adsorption-desorption studies revealed that the prepared GO was macro-porous while all other samples were mesoporous. MGO was found to have the highest BET surface area of about 108.375 m²/g. These results indicate that the prepared nanomaterials may serve the purpose of effectively adsorbing the heavy metal ions from an aqueous solution.



Article History

Received: 24 January 2023

Accepted: 14 March 2023

Keywords

Adsorption;
Graphene Oxide;
Heavy Metals;
Nanomaterials;
Titanium Dioxide.

Introduction

The discharge of heavy metals into aquatic ecosystems has raised global concerns over the past few decades. These contaminants are introduced

into water bodies through effluents from various industries, including paper and pulp, petrochemicals, automobiles, and battery manufacturing. While several methods, such as precipitation, ion exchange,

CONTACT Kiran Jeet ✉ kiranjeet@pau.edu 📍 Electron Microscopy & Nanoscience Laboratory, Punjab Agricultural University, Ludhiana, Punjab, India.



© 2023 The Author(s). Published by Enviro Research Publishers.

This is an Open Access article licensed under a Creative Commons license: Attribution 4.0 International (CC-BY).

Doi: <http://dx.doi.org/10.13005/msri/200107>

reverse osmosis, and membrane filtration, have been employed to remove heavy metals. Most of these methods have drawbacks, such as high cost, low efficiency, and sludge generation (Kumar *et al.*, 2019). Additionally, they fail to meet the demand for water resources, particularly for large volumes. Adsorption, on the other hand, is a simple, economical, and adaptable method in terms of unit design. Natural and synthetic adsorbents, such as clay, activated carbon, mesoporous silica, and resin, have been used to treat heavy metal-contaminated water. However, separating and regenerating these adsorbents from wastewater poses a significant challenge. Therefore, there is a need to develop novel adsorbents with high adsorption capacity and quick separation from large volumes of water (Almomani *et al.*, 2019). Recently, nanomaterials, particularly carbon-based and metal oxide-based ones, have emerged as promising adsorbents for heavy metal ions due to their high specific surface area, surface-to-volume ratio, and concentrated pore size distribution (Khan *et al.*, 2013; Qu *et al.*, 2015). Among these, graphene oxide (GO), a carbon-based nanomaterial, has received widespread attention (Yan *et al.*, 2014, Majumder P, Gangopadhyay R. 2022). GO consists of a hexagonal network of covalently bonded carbon atoms with oxygen-containing functional groups, such as hydroxyl, epoxy, lactone, quinone, phenol, anhydride, carbonyl, ether, and carboxyl groups, attached to various sites, which facilitate the binding of positively charged metal ions to its surface (Guerrero-Fajardo *et al.*, 2020; Zhao *et al.*, 2011). However, GO's hydrophilicity and tendency to agglomerate during its application and storage make it challenging to separate, even after saturation adsorption (Liu *et al.*, 2015; Sun *et al.*, 2015). To address these issues, GO can be magnetized, for example, with iron oxides. Nano-sized iron oxides exhibit superparamagnetism, low toxicity, chemical inertness, and the ability to immobilize various adsorbents on their surface (Jawed *et al.*, 2020). The magnetized GO can be easily separated using an external magnetic field (Lingamdinne *et al.*, 2019). Another category of nanomaterials that has shown favourable adsorption towards heavy metals is nano-sized metal oxides (Hua *et al.*, 2012). Functionalizing GO with metal oxides largely increases the electronegative charge on its surface thereby improving metal removal efficiency (Jawed *et al.*, 2020). The inclusion of active materials such as manganese dioxide

(Xiang *et al.*, 2018), iron oxide (Tian *et al.*, 2017), and titanium dioxide (Liu *et al.*, 2016) have sparked a profound interest in the field of adsorption as the metallic compounds could improve the adsorption performance by providing more active sites (Lai *et al.*, 2020). Titanium dioxide nanoparticles are widely used as an adsorbent for heavy metal ions due to their low cost, stability, and non-toxicity towards human beings and the environment (Seidlerová *et al.*, 2016). Here in this work the synthesis of adsorbents such as Graphene Oxide (GO), Magnetic Graphene Oxide (MGO), Titanium Dioxide (TiO_2), and their composites GO- TiO_2 , and MGO- TiO_2 has been reported. GO- TiO_2 is synthesized keeping in view the favourable properties of both GO and TiO_2 . MGO- TiO_2 nanocomposites are synthesized aiming at integrating the advantages of all the components – GO, TiO_2 along with magnetic properties of iron oxide for the added advantage of easier regeneration of adsorbents and improve the overall adsorption efficiency.

Material and Methods

Graphite fine powder extra pure of size 10-30 nm was procured from Loba Chemicals, sulfuric acid (H_2SO_4), potassium permanganate (KMnO_4), phosphoric acid (H_3PO_4), ferrous ammonium sulfate hexahydrate [$(\text{NH}_4)_2\text{Fe}(\text{SO}_4)_2 \cdot 6\text{H}_2\text{O}$], ammonium ferric sulfate dodecahydrate [$(\text{NH}_4)_2\text{Fe}(\text{SO}_4)_2 \cdot 10\text{H}_2\text{O}$], aqueous ammonia (NH_4OH) (weight 25%), hydrogen peroxide (H_2O_2), isopropyl alcohol (IPA), titanium isopropoxide (TTIP), isopropanol, HCl, and anhydrous ethanol were procured from Molychem, and were of analytical grade and used without any further purification.

Synthesis of Adsorbents

GO was prepared by the modified Hummer's method. Graphite powder was added into a mixture of concentrated H_2SO_4 and H_3PO_4 in the ratio of 9:1 under continuous stirring followed by the addition of KMnO_4 to bring about the oxidation. The mixture was stirred continuously till the color changed to purple. Then the mixture was cooled down to room temperature and an ice water mixture and H_2O_2 were added to stop the reaction. A yellow-colored solution was obtained which was then sonicated to bring about the complete exfoliation of graphite oxide. Then the solution was centrifuged once with HCl and many times with distilled water until a neutral pH was obtained. Finally, solid GO was

obtained by vacuum drying in an oven and grinding using a pestle and mortar (Kaur and Jeet 2017).

The observations recorded during the synthesis of GO are given in figure 1.

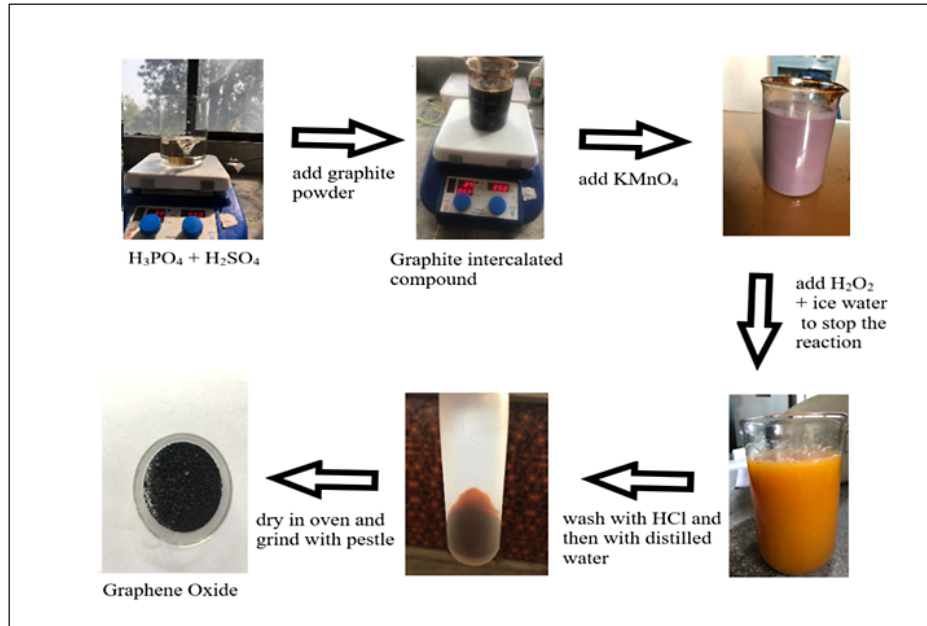


Fig. 1: Observations recorded during the synthesis of Graphene Oxide

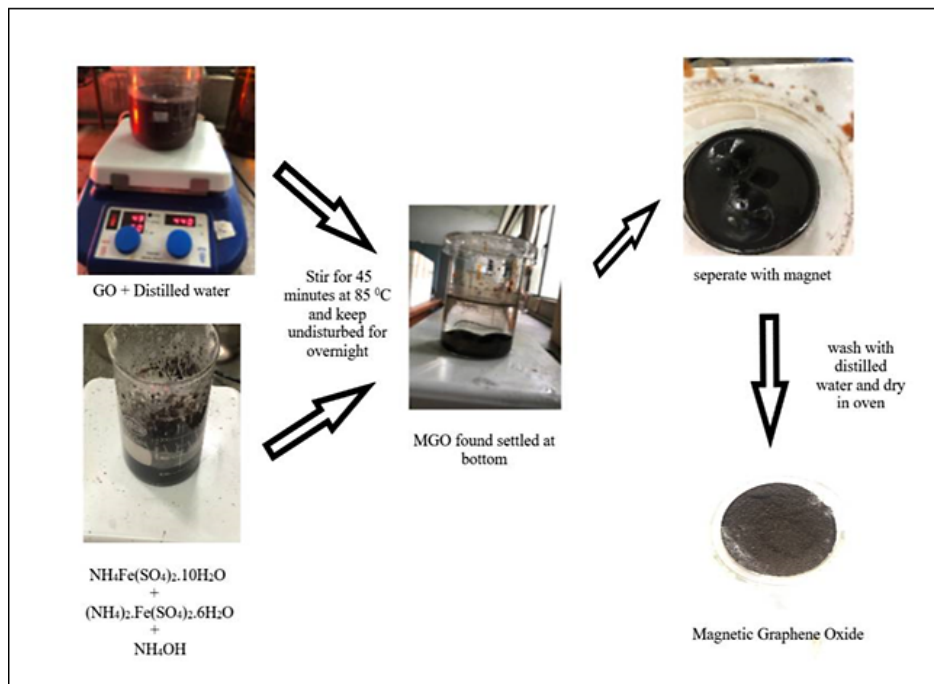


Fig. 2: Observations recorded during the synthesis of MGO

MGO was prepared by the co-precipitation of iron oxide nanoparticles on the surface of GO. A dispersion of GO was prepared by adding a small amount of prepared GO in 100 ml of double-distilled water and sonicating it for an hour. Then, 10.7 g of ferric ammonium sulfate and 5.8 g of ferrous ammonium sulfate were added to 100 ml of double-distilled water followed by the rapid addition of 10 ml of aqueous ammonia. The solution was then kept under stirring and GO suspension was slowly added to this solution after that the stirring was continued for about 45 minutes at 85 °C and then the solution was kept undisturbed overnight. Finally, MGO was separated with a magnet and washed thrice with distilled water and anhydrous ethanol respectively. Subsequently, MGO was kept in an oven at 70

°C for drying (Deng *et al.*, 2013, Yi *et al.* 2021). The observations recorded during the synthesis of MGO are given in figure 2.

Titanium Dioxide was prepared by a wet chemical method. 10 ml of TTIP was added into a solution containing ethanol and double distilled water in the ratio of 7:1 under constant stirring. The stirring was further continued at room temperature until a thick paste with lots of nanoparticles was obtained, which were then separated by centrifugation with distilled water. The nanoparticles were then calcined and stored in an airtight container (Tamilselvi *et al.*, 2016, Mironyukl *et al.* 2020). The observations recorded during the synthesis of TiO₂ are given in figure 3.

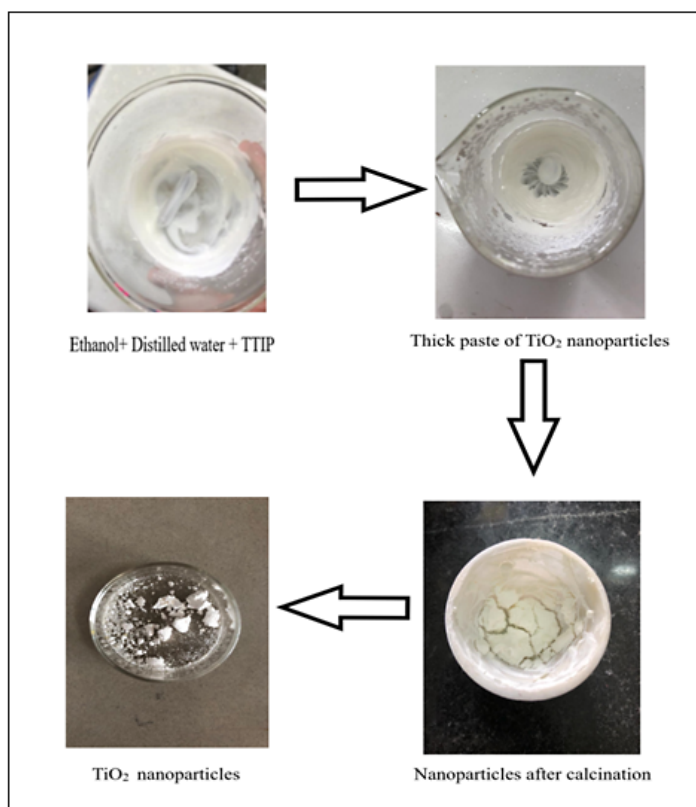


Fig. 3: Observations recorded during the synthesis of TiO₂

GO-TiO₂ nanocomposite was prepared by the sol-gel process. A small amount of the prepared GO was added into the double distilled water and was sonicated to re-exfoliate GO. Afterward, a mixture of isopropanol and TTIP in the ratio of 4:1 was dropped into the GO solution under continuous stirring for the

crystallization of TiO₂ Nanoparticles. The precipitates were washed, filtered with water and ethanol, and dried in the oven. Finally, GO-TiO₂ nanohybrids were obtained by calcination at 400°C (Sakulpaisan *et al.*, 2016). The observations recorded during the synthesis of GO-TiO₂ are given in figure 4.

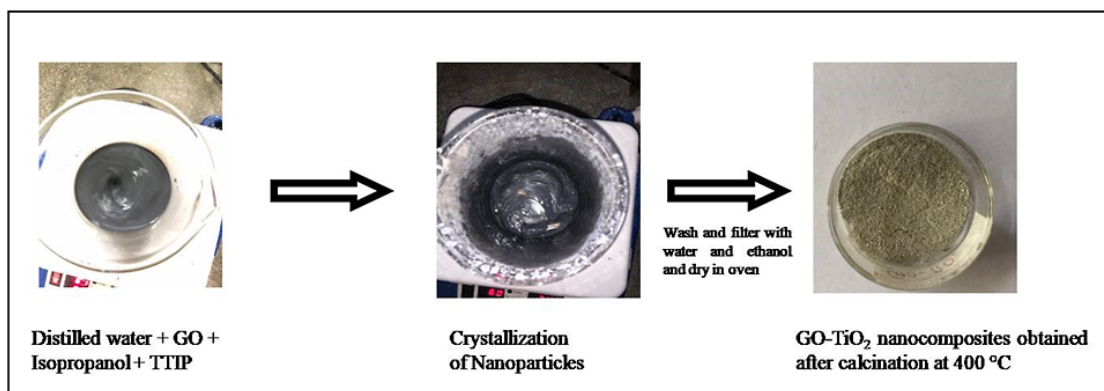


Fig. 4: Observations recorded during the synthesis of GO-TiO₂

For the preparation of MGO-TiO₂ nanocomposite, the prepared GO and TiO₂ nanoparticles were separately dispersed in double-distilled water and were sonicated for about an hour. Then (NH₄)₂Fe(SO₄)₂·6H₂O and (NH₄)₂Fe(SO₄)₂·10H₂O were dispersed in distilled water and 10 ml of aqueous ammonia was quickly added to this solution, as in the preparation of MGO. Afterward,

this solution and TiO₂ dispersion were simultaneously added to the GO dispersion under vigorous stirring. The stirring was further continued at 850C for 45 minutes and kept overnight at room temperature. The rest of the procedure of obtaining nanoparticles was the same as that in the case of MGO (Chang *et al.*, 2015). The pictorial representation of MGO-TiO₂ synthesis is given in figure 5.

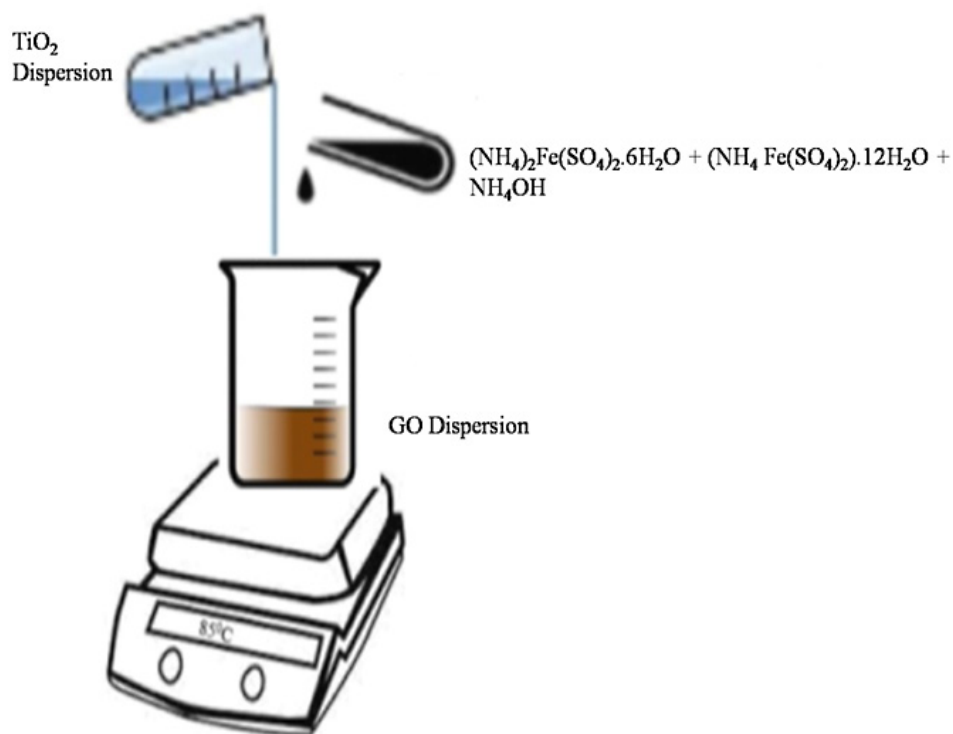


Fig. 5: Pictorial representation of MGO-TiO₂ synthesis

Characterization

The surface area of the prepared nanomaterials was examined by BET N_2 adsorption-desorption analysis using Micromeritics ASAP 2020 volumetric adsorption analyzer installed at Emerging Life Sciences, Guru Nanak Dev University, Amritsar, Punjab, India. Before each analysis, each sample was degassed for 4-6 hours at 2000C. For the determination of the elemental composition and functional groups present the prepared samples were analyzed using Perkin Elmer Fourier Transform Infrared Spectrometer installed at Central Instrumentation Facility, Lovely Professional University, Phagwara, Punjab, India. The prepared samples were viewed under Transmission Electron Microscopy (TEM) installed at the Electron Microscopy and Nanoscience Lab, Punjab Agricultural University, Ludhiana, Punjab, India, to study their structural and morphological properties.

Results and Discussions

BET N_2 Adsorption-Desorption Analysis

Magnetic Graphene Oxide was found to have the largest surface area of 108.3750 m^2/g .

The magnetization of GO appeared to increase its surface area, as evidenced by the larger surface area of MGO compared to GO. The surface areas of both the nanocomposites ie. GO-TiO₂ and MGO-TiO₂ were less than that of MGO which showed that the substitution of graphene oxide with titanium dioxide decrease its surface area. Due to the agglomeration of individual nanoparticles, the surface area of TiO₂ nanoparticles was only 4.42 m^2/g . The extremely high calcination temperature may have contributed to the high average particle size of TiO₂ particles. As a result, the individual TiO₂ nanoparticles were agglomerated which was also evident from the TEM micrograph of TiO₂ nanoparticles. The pore diameters of the synthesized samples confirmed the presence of mesopores as per the IUPAC classification except for GO which was found to be macroporous (Thommes *et al.*, 2015). The BET surface areas, pore sizes, and pore volume distribution of the synthesized samples are given in Table 1.

Table 1: BET surface areas, pore sizes, and pore volume distribution of the synthesized samples

Adsorbent	BET surface area (m^2/g)	Pore width (nm) By BET method	Pore volume (cm^3/g) By BET method	Average particle size (nm)	BJH adsorption average pore diameter (nm)
Graphene Oxide (GO)	35.8220	31.97	0.286316	167.4947	51.7066
Magnetic Graphene Oxide (MGO)	108.3750	9.77	0.264600	55.36	9.67
Titanium Dioxide (TiO ₂)	4.4288	268.67	0.297472	1354.76	46.755
GO-TiO ₂	106.1106	16.89	0.448001	56.545	13.91
MGO-TiO ₂	81.3364	19.71251	0.400836	73.77	23.63

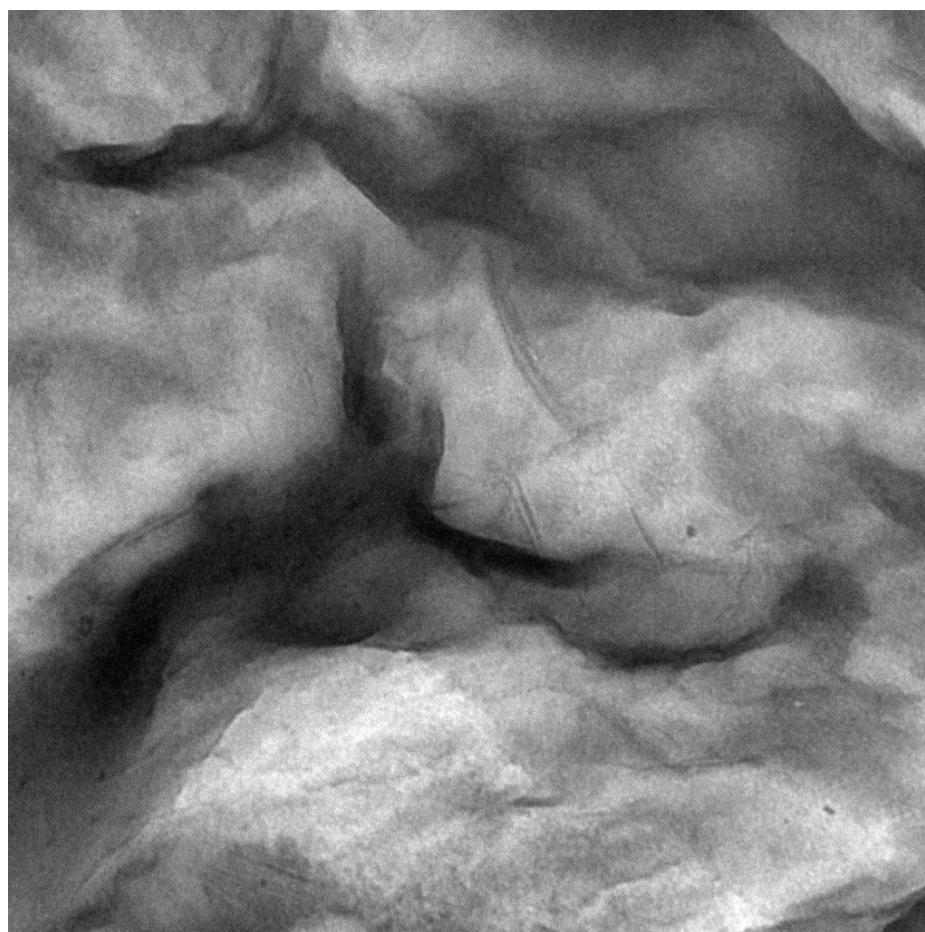
Transmission Electron Microscopy

Figure 6 shows the TEM micrographs of the prepared samples. The TEM micrograph of GO captured at 500 nanometers (Figure 6a) reveals a layered-wrinkled structure with many folds on it, which may be attributed to various oxygen-containing functional groups (Liu *et al.*, 2015; Deng *et al.*, 2013, Nhlane *et al.* 2021). The TEM micrograph of MGO (Figure 6b) was captured at 100 nm and depicts the homogeneous distribution of iron-oxide nanoparticles on the surface of GO. The

average diameter of MGO nanoparticles determined using Image J software was found to be 24.58 nm (Deng *et al.*, 2013). The TEM micrograph of TiO₂ nanoparticles (Figure 6c) reveals that the formed TiO₂ nanoparticles are almost spherical and are aggregated to some extent. The average diameter of TiO₂ nanoparticles was found to be 35.51 nm. The TEM micrograph of GO-TiO₂ nanocomposite (Figure 6d) shows the successful deposition of TiO₂ nanoparticles on the layered structure of GO (Ibrayev *et al.*, 2019). The TEM images of the MGO-

TiO₂ nanohybrid (Figure 6e) depict the presence of iron-oxide nanoparticles, some iron rods, and TiO₂ nanoparticles on the surface of GO, showing the successful stacking of all the components.

The crumpled structure of GO sheets enables the binding of nanoparticles onto their surface (Chang *et al.*, 2015; Jo & Selvam, 2015).



File name=sample_Z0_002.bmp
Image date=2021/08/13 11:33:58
Image number=1
Image comment=Hitachi TEM system.
Calibration=1.75 nm/pixel at x:10.0k
Magnification=x10.0k
Lens mode=Zoom-1
Spot number=5
Image rotation=0°
Acc. voltage=80kV
Emission=11.3µA
Stage.X=405 Y=198 Tilt angle=3.8
Azim angle=0.0

Fig. 6a): TEM micrograph of GO

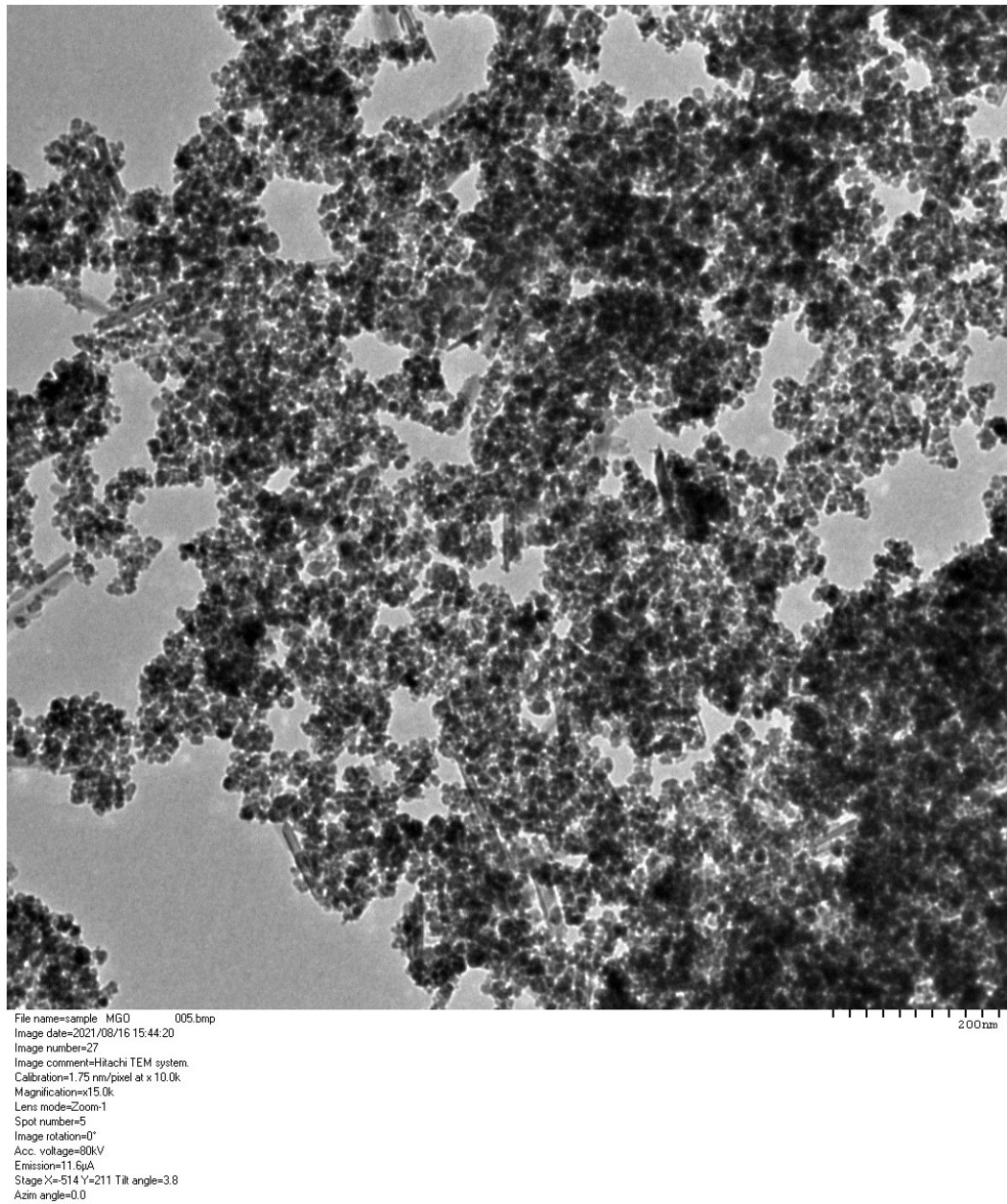
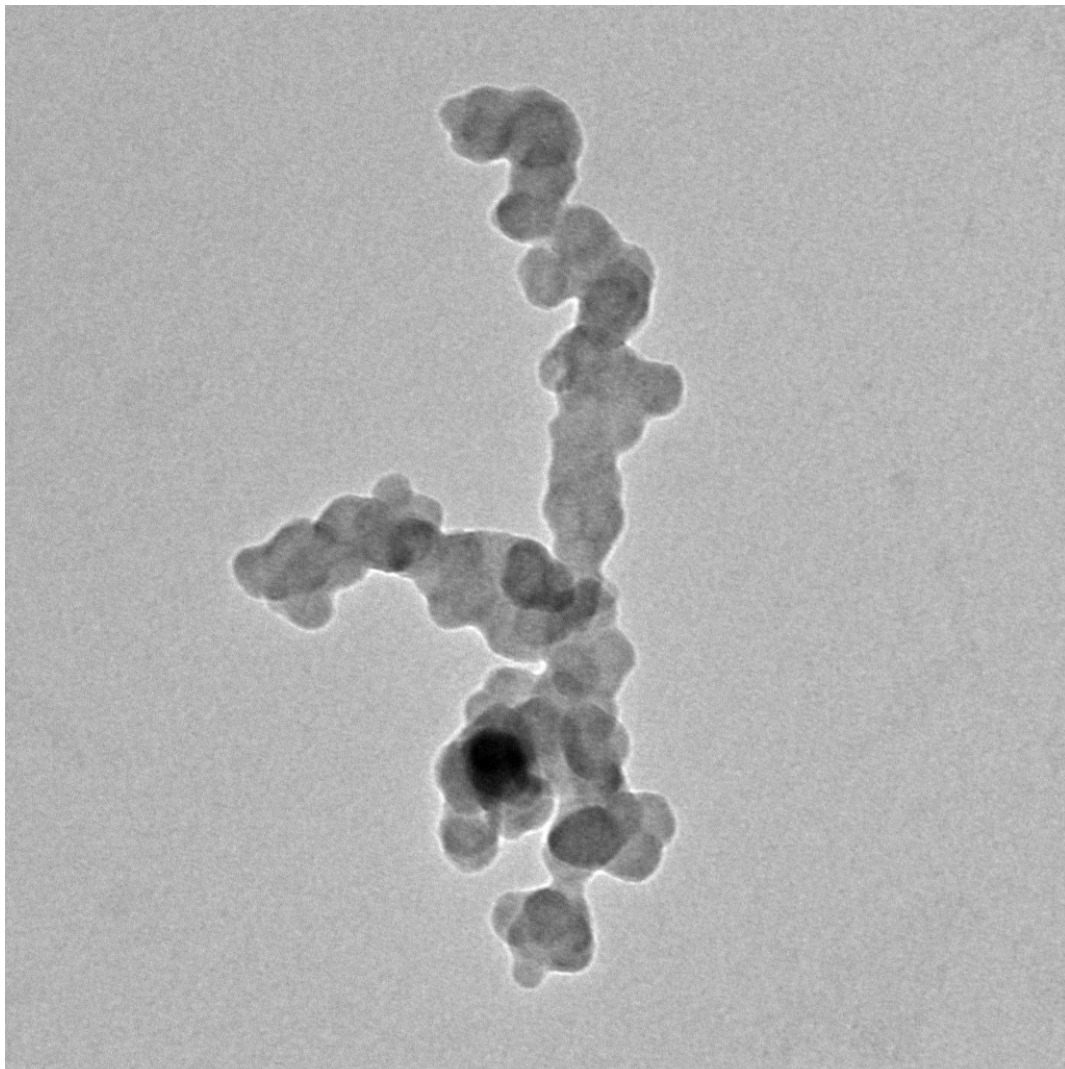
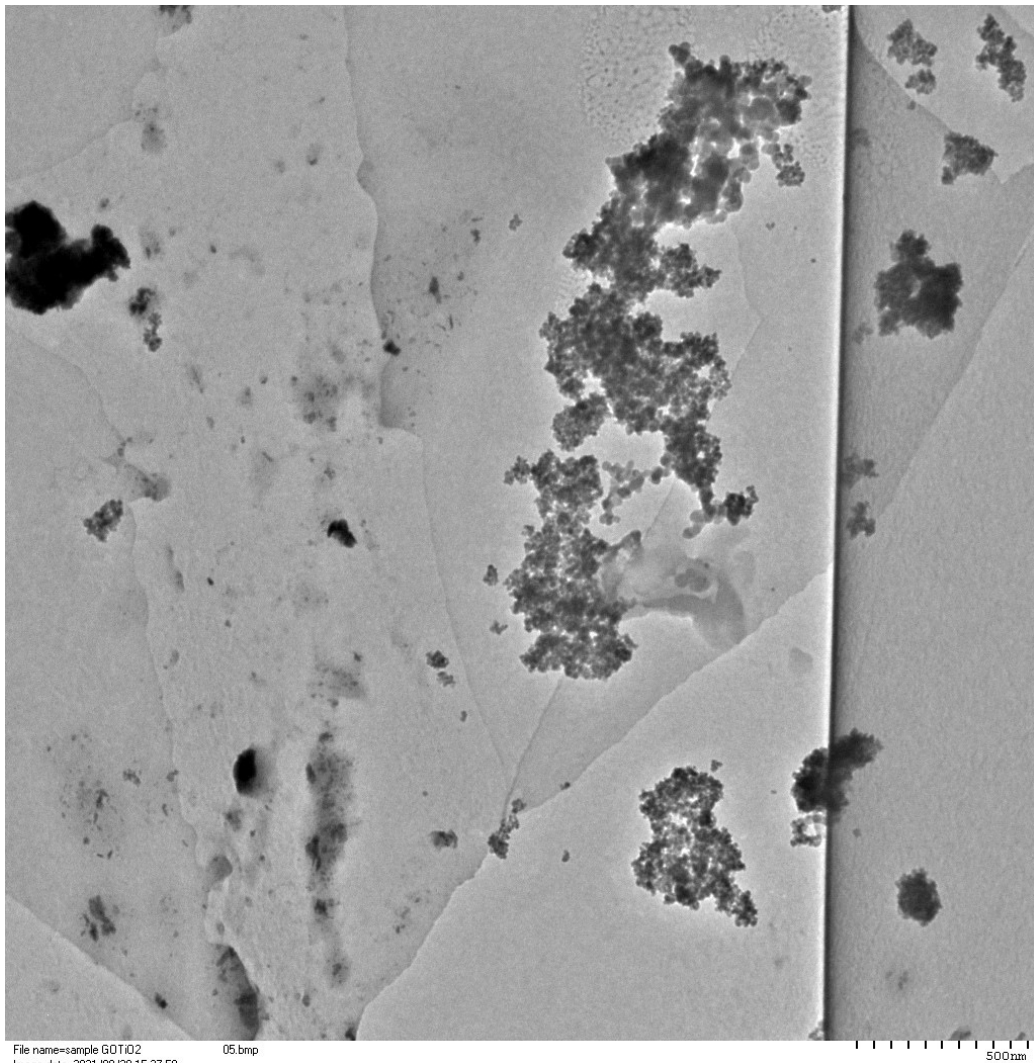


Fig. 6b): TEM micrograph of MGO



File name=sample TiO2 002.bmp
Image date=2021/08/16 15:56:22
Image number=32
Image comment=Hitachi TEM system.
Calibration=1.75 nm/pixel at x 10.0k
Magnification=x30.0k
Lens mode=Zoom-1
Spot number=5
Image rotation=0°
Acc. voltage=80kV
Emission=11.6µA
Stage X=196 Y=725 Tilt angle=3.8
Azim angle=0.0

Fig. 6c): TEM micrograph of TiO2



File name=sample G0TiO2 05.bmp
Image date=2021/08/20 15:27:50
Image number=59
Image comment=Hitachi TEM system.
Calibration=1.75 nm/pixel at x10.0k
Magnification=x6.0k
Lens mode=Zoom-1
Spot number=5
Image rotation=0°
Acc. voltage=80kV
Emission=11.8µA
Stage X=-147 Y=-9 Tilt angle=3.8
Azim angle=0.0

Fig. 6d): TEM micrograph of GO-TiO₂

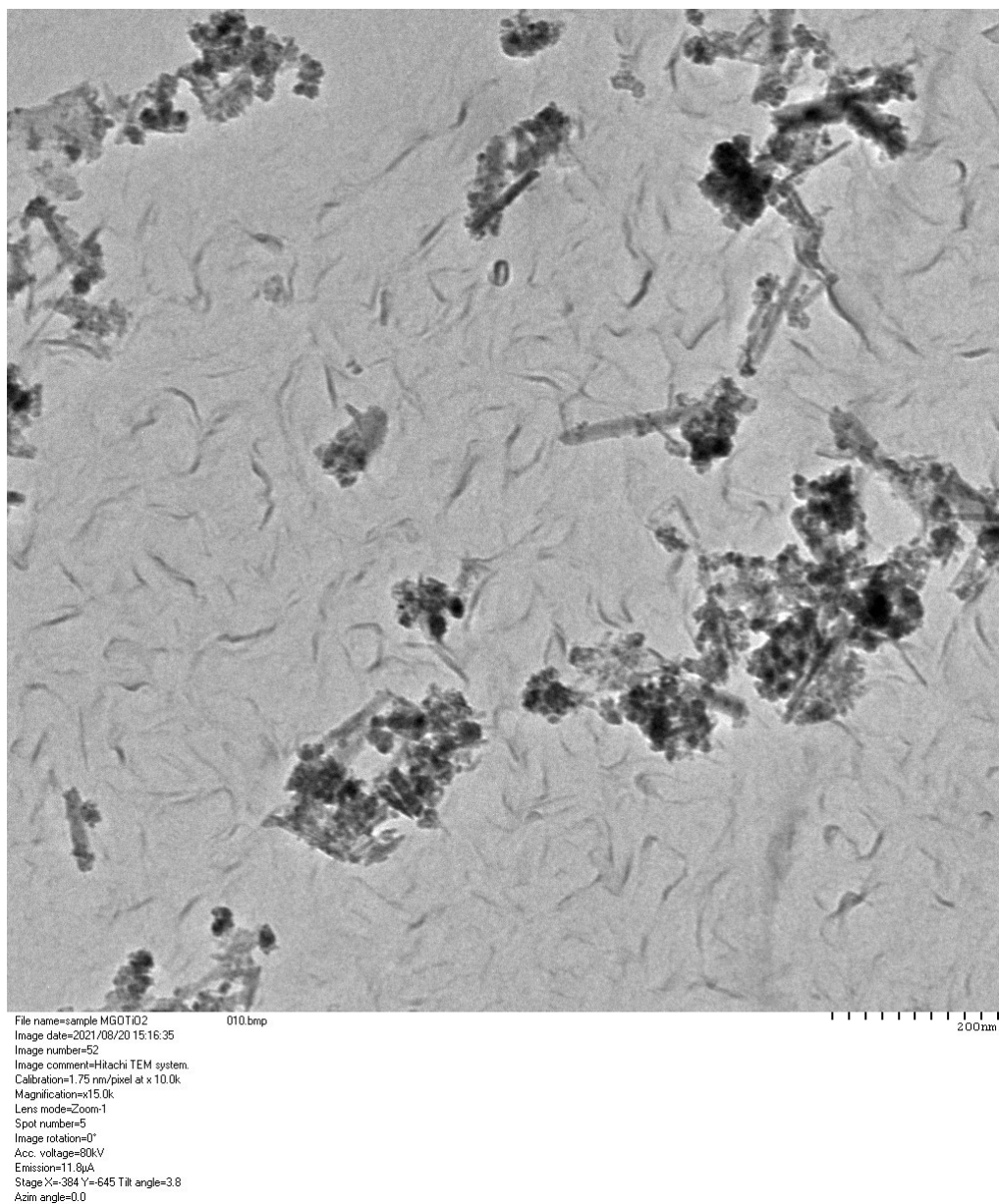


Fig. 6e): TEM micrograph of MGO-TiO₂

FT-IR Spectroscopy

The FT-IR spectra of the prepared samples are presented in Figure 7. The FT-IR spectrum of GO displayed a broad band at 3225.37 cm⁻¹, which can be attributed to the presence of water adsorbed on the surface of GO or to the structural hydroxyl groups (-COH and -COOH) of GO. Additionally, a band

at 1722.77 cm⁻¹ was observed, which is characteristic of the vibrations of the C=O group, and a band at 1046.22 cm⁻¹ was due to C-O stretching vibrations of the alkoxy group (Sitko *et al.*, 2013).

The FT-IR spectrum of MGO exhibited a band at 3203.39 cm⁻¹, which can be attributed to the O-H

stretching vibrations. Additionally, a band at 551.62 cm^{-1} was observed, which is due to Fe-O stretching vibrations. The band at 890.95 cm^{-1} supports the

deposition of iron nanoparticles on the surface of GO (Liu *et al.*, 2015; Sun *et al.*, 2018).

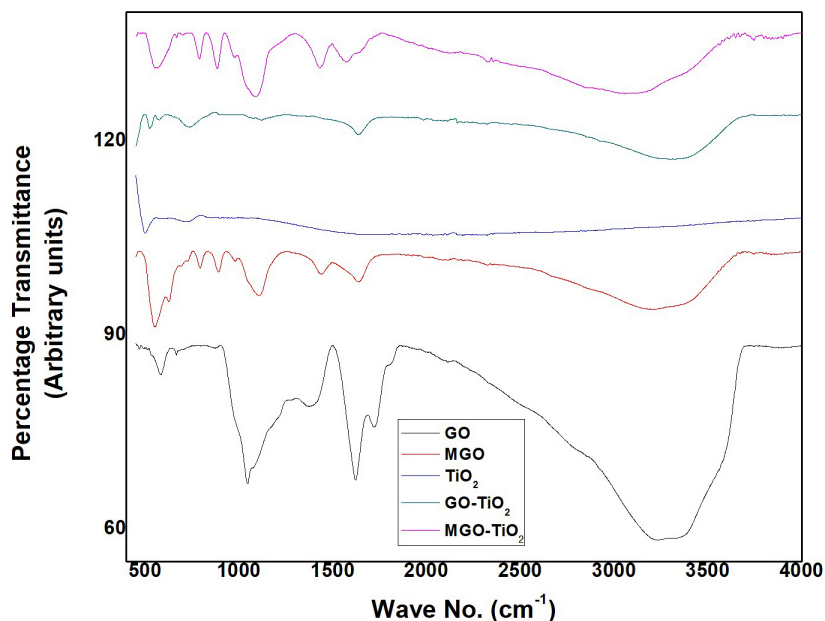


Fig. 7: FT-IR spectra of the prepared samples

The FT-IR spectrum of TiO_2 exhibited only one major peak at 499 cm^{-1} , which is characteristic of Ti-O-Ti bonds (Bok-Badura *et al.*, 2017). The FT-IR spectrum of GO- TiO_2 showed bands at 1635.26 cm^{-1} and 3387 cm^{-1} , which are characteristic of aromatic groups and O-H stretching vibrations, respectively. Additionally, a band at 523.51 cm^{-1} was observed, which corresponds to the Ti-O-Ti vibrations (Sakulpaisan *et al.*, 2016; Kurniawan *et al.*, 2020).

The FT-IR spectrum of MGO- TiO_2 displayed bands at 3058 cm^{-1} , 1578 cm^{-1} , 1086 cm^{-1} , and 788 cm^{-1} , which are attributed to the adsorbed water content on the GO surface, C=C vibrations, C-O vibrations, and C-O-Ti vibrations, respectively. The band at 884 cm^{-1} can be attributed to the covalent bonding of Fe_3O_4 nanoparticles on the GO surface. The lowering of the carbonyl band of GO to 1431 cm^{-1} indicates the successful deposition of TiO_2 and Fe_3O_4 nanoparticles on the GO surface (Zhang *et al.*, 2015).

Conclusion

The morphologies and size of the prepared nanomaterials were determined using transmission electron microscopy. TEM micrograph of GO depicted the formation of the layered structure of GO with many folds which might be attributed to the presence of oxygen-containing functionalities, TiO_2 micrograph depicted the formation of large agglomerates of TiO_2 particles. MGO- TiO_2 revealed the deposition of iron oxide nanoparticles and TiO_2 nanoparticles on the surface of GO. From the TEM micrographs the approximate sizes of MGO and TiO_2 nanoparticles were found to be about 24.58 and 35.51 nm respectively. FT-IR spectra of the synthesized nanomaterials depict the presence of required functional groups on their respective surfaces. N_2 adsorption-desorption studies exhibited that MGO was having the highest surface area (108.3750 m^2/g), and the prepared GO was macroporous while all other samples were mesoporous. Thus, the successful preparation of the adsorbents was confirmed.

Transmission electron microscopy was used to measure the produced nanomaterials' sizes and morphologies. A TiO₂ micrograph showed the formation of huge agglomerates of TiO₂ particles, and a TEM image of GO showed the development of a layered structure with many folds that may be explained by the presence of oxygen-containing functionalities. TiO₂ and iron oxide nanoparticles were found to have been deposited on the surface of GO by MGO-TiO₂. The approximate diameters of MGO and TiO₂ nanoparticles were determined from the TEM micrographs to be around 24.58 and 35.51 nm, respectively. The presence of necessary functional groups on the surfaces of the synthesized nanomaterials is shown in their FT-IR spectra. Studies on the N₂ adsorption-desorption of several materials showed that MGO had the greatest surface area (108.3750 m²/g), and that the produced GO was macroporous whereas all other samples were mesoporous. Thus, the adsorbents' successful preparation was verified. The results of the study provide information about the functional groups present in nanomaterials, which further aids in determining the heavy metal contamination

that can be eliminated from aqueous medium, making the study highly beneficial for the synthesis of real-time filters. Moreover, surface area-related information offers binding site-related information. Better adsorption capability is demonstrated by higher surface area. The usage of GO as an adsorbent indicated an increase in the strength of the filtration material.

Acknowledgments

We sincerely thank the Department of Science and Technology for providing us research grant under the Promotion of University Research and Scientific Excellence (PURSE) grant scheme for carrying out the research work of this manuscript.

Funding

Department of Science and Technology (DST) under research grant Promotion of University Research and Scientific Excellence (PURSE).

Conflict of interest

On behalf of all authors, the corresponding author states that there is no conflict of interest.

References

1. Almomani F, Bhosale R, Khraisheh M, kumar A, Almomani T (2019) Heavy Metal ions removal from industrial wastewater using magnetic nanoparticles (MNP), *Appl. Surf. Sci.* doi: <https://doi.org/10.1016/j.apsusc.2019.144924>
2. Argun M E and Dursun S (2008) A new approach to modification of natural adsorbent for heavy metal adsorption. *Bioresour Technol* 99 2516-2527 <https://doi.org/10.1016/j.biortech.2007.04.037>.
3. Bok-Badura J, Jakóbk-Kolon A, Karoń K and Mitko K (2017) Sorption studies of heavy metal ions on pectin-nano-titanium dioxide composite adsorbent in *Sep Sci Technol* 53 1034-1044 <http://dx.doi.org/10.1080/01496395.2017.1329840>.
4. Chang Y N, Ou X M, Zeng G M, Gong J L, Deng C H, Jiang Y, Liang J, Yu G Q, Liu H Y and He X (2015) Synthesis of magnetic graphene oxide-TiO₂ and their antibacterial properties under solar irradiation in *Appl Surf Sci* 343 1-10 <https://doi.org/10.1016/j.apsusc.2015.03.082>.
5. Deng J H, Zhang X R, Zeng G M, Gong J L, Niu Q Y and Liang J (2013) Simultaneous removal of Cd(II) and ionic dyes from aqueous solution using magnetic graphene oxide nanocomposite as an adsorbent in *J Chem Eng* 226 189-200 <https://doi.org/10.1016/j.cej.2013.04.045>.
6. Guerrero-Fajardo C A, Giraldo L and Moreno-Piraján J C (2020) Preparation and Characterization of Graphene Oxide for Pb(II) and Zn(II) Ions Adsorption from Aqueous Solution: Experimental, Thermodynamic and Kinetic Study in *Nanomaterials* 10(6) 1022 <https://doi.org/10.3390/nano10061022>.
7. Hua M, Zhang S, Pan B, Zhang W, Lv L and Zhang Q (2012) Heavy metal removal from water/wastewater by nanosized metal oxides: A review in *J Hazard Mater* 211-212 317-331 <https://doi.org/10.1016/j.jhazmat.2011.10.016>.
8. Ibrayev N, Zhumabekov A, Ghyngazov S and Lysenko E (2019) Synthesis and study of the properties of nanocomposite materials TiO₂-GO and TiO₂-rGO. *Mater Res Express*, 6 1-10

- <https://doi.org/10.1088/2053-1591/ab51a3>.
9. Jawed A, Saxena V and Pandey L M (2020) Engineered nanomaterials and their surface functionalization for the removal of heavy metals: A review in *J Water Process Eng* 33 101009 <https://doi.org/10.1016/j.jwpe.2019.101009>.
 10. Jo W K and Selvam N C S (2015) Synthesis of GO supported Fe₂O₃-TiO₂ nanocomposites for enhanced visible-light photocatalytic applications in *Dalton Trans* 44 16024-16035 <https://doi.org/10.1039/C5DT02983J>.
 11. Kaur K and Jeet K (2017) Electrical conductivity of water- based nanofluids prepared with graphene – carbon nanotube hybrid. Fuller Nanotub in *Carbon Nanostructures* 2 726-734 <https://doi.org/10.1080/1536383X.2017.1389906>.
 12. Khan M A, Gee E, Choi J, Kumar M, Jung W, Timmes T C, Kim H-C, & Jeon B-H (2013) Adsorption of cobalt onto graphite nanocarbon-impregnated alginate beads: equilibrium, kinetics, and thermodynamic studies in *Chem Eng. Commun* 201 (3) 403–418 <https://doi.org/10.1080/00986445.2013.773426>.
 13. Kumar M, Chung J S and Hur S H (2019) Graphene Composites for Lead Ions Removal from Aqueous Solutions in *Appl Sci* 9(14) 1-30 <https://doi.org/10.3390/app9142925>.
 14. Kurniawan T A, Mengting Z, Fu D, Yeap S K, Othman M H D, Avtar R and Ouyang T (2020) Functionalizing TiO₂ with graphene oxide for enhancing photocatalytic degradation of methylene blue (MB) in contaminated wastewater in *J Environ Manage* 270 110871 <https://doi.org/10.1016/j.jenvman.2020.110871>.
 15. Lai K C, Lee L Y, Hiew B Y Z, Thangalazhy-Gopakumar S, Gan S (2020) Facile synthesis of xanthan biopolymer integrated 3D hierarchical graphene oxide/titanium dioxide composite for adsorptive lead removal in wastewater in *Bioresource Technology* 309 123296. <https://doi.org/10.1016/j.biortech.2020.123296>.
 16. Lingamdinne L P, Koduru J R and Karri R R (2019) A comprehensive review of applications of magnetic graphene oxide based nanocomposites for sustainable water purification in *J Environ Manage* 231 622-634 <https://doi.org/10.1016/j.jenvman.2018.10.063>.
 17. Liu J, Ge X, Ye X, Wang G, Zhang H, Zhou H, Zhang Y and Zhao H (2016) 3D graphene/ δ -MnO₂ aerogels for highly efficient and reversible removal of heavy metal ions in *J Mater Chem A* 4 1970-1979 <https://doi.org/10.1039/C5TA08106H>.
 18. Liu L, Zhang Y, He Y, Xie Y, Huang L, Tan S and Cai X (2015) Preparation of montmorillonite-pillared graphene oxide with increased single- and co-adsorption towards lead ions and methylene blue in *RSC Adv* 5 3965-3973 <https://doi.org/10.1039/C4RA13008A>.
 19. Majumder P, Gangopadhyay R (2022) Evolution of graphene oxide (GO)-based nanohybrid materials with diverse compositions: an overview. *RSC Adv* 12:5686–5719 <https://doi.org/10.1039/D1RA06731A>
 20. Mironyukl. F., SoltysL. M., TatarchukT. R., & SavkaK. O. (2020). Methods of Titanium Dioxide Synthesis (Review). *Physics and Chemistry of Solid State*, 21(3), 462-477. <https://doi.org/10.15330/pcss.21.3.462-477>
 21. Nhlane D, Richards H, Etale A (2021) Facile and green synthesis of reduced graphene oxide for remediation of Hg(II)-contaminated water. *Mater Today Proc* 38:737–742 <https://doi.org/10.1016/j.matpr.2020.04.163>
 22. Qu J, Zhang Q, Xia Y, Cong Q and Luo C (2015) Synthesis of carbon nanospheres using fallen willow leaves and adsorption of Rhodamine B and heavy metals by them in *Environ Sci Pollut Res Int* 22 1408–1419 <https://doi.org/10.1007/s11356-014-3447-x>.
 23. Roy A and Bhattacharya J (2015) Nanotechnology in industrial wastewater treatment. IWA Publishing, London, UK
 24. Sakulpaisan S, Vongsetskul T, Reamouppatum S, Luangkachao L, Tantirungrotechai J and Tangboriboonrat P (2016) Titania-functionalized graphene oxide for an efficient adsorptive removal of phosphate ions in *J Environmental Management* 167 99–104. <https://doi.org/10.1016/j.jenvman.2015.11.028>.
 25. Seidlerová J, Šafařík I, Rozumová L, Šafaříková M and Motyka O (2016) TiO₂-Based Sorbent of Lead Ions in *Procedia Mater Sci* 12 147 – 152 <https://doi.org/10.1016/j.mspro.2016.03.026>.
 26. Sitko R, Turek E, Zawisza B, Malicka E, Talik E, Heimann J, Gagor A, Feist B and Wrzalik R, (2013) Adsorption of divalent metal ions from aqueous solutions using graphene oxide in *Dalton Trans* 42 5682-5689 <https://doi.org/10.1039/C3DT00000A>.

- org/10.1039/C3DT33097D.
27. Sun J, Liang Q, Han Q, Zhang X and Ding M (2015) One-step synthesis of magnetic graphene oxide nanocomposite and its application in magnetic solid phase extraction of heavy metal ions from biological samples in *Talanta* 132 557-563 <https://doi.org/10.1016/j.talanta.2014.09.043>.
 28. Sun M, Li P, Jin X, Ju X, Yan W, Yuan J and Xing C (2018) Heavy metal adsorption onto graphene oxide, amino group on magnetic nanoadsorbents and application for detection of Pb(II) by strip sensor in *Food Agric Immunol* 29 1053-1073 <https://doi.org/10.1080/09540105.2018.1509946>.
 29. Tamilselvi S, Asaithambi M, and Sivakumar P (2016) Nano-TiO₂-loaded activated carbon fiber composite for photodegradation of a textile dye in *Desalination water treat* 57 (33) 15495-15502 <https://doi.org/10.1080/19443994.2015.1071684>.
 30. Thommes M, Kaneko K, Neimark A, Olivier J, Rodriguez-Reinoso F, Rouquerol J and Sing K (2015) Physisorption of gases, with special reference to the evaluation of surface area and pore size distribution (IUPAC Technical Report) in *Pure Appl Chem* 87 (9-10) 1051-1069 <https://doi.org/10.1515/pac-2014-1117>.
 31. Tian C, Zhao J, Zhang J, Chu S, Dang Z, Lin Z and Xing B (2017) Enhanced removal of roxarsone by Fe₃O₄@3D graphene nanocomposites: synergistic adsorption and mechanism in *Environ Sci: Nano* 4 (11) 2134-2143 <https://doi.org/10.1039/C7EN00758B>.
 32. Xiang C, Guo R, Lan J, Jiang S, Wang C, Du Z and Cheng C (2018) Self-assembling porous 3D titanium dioxide-reduced graphene oxide aerogel for the tunable absorption of oleic acid and RhodamineB dye in *J Alloys Compd* 735 246-252 <http://dx.doi.org/10.1016/j.jallcom.2017.11.034>.
 33. Yan H, Li H, Tao X, Li K, Yang H, Li A, Xiao S, and Cheng R (2014) Rapid Removal and Separation of Iron(II) and Manganese(II) from Micropolluted Water Using Magnetic Graphene Oxide in *ACS Appl. Mater. Interfaces* 6 (12) 9871-9880 <https://doi.org/10.1021/am502377n>.
 34. Yi He, Chen Yi, Xiliu Zhang, Wei Zhao, Dongsheng Yu (2021), Magnetic graphene oxide: Synthesis approaches, physicochemical characteristics, and biomedical applications, *TrAC Trends in Analytical Chemistry*, Volume 136, 116191, <https://doi.org/10.1016/j.trac.2021.116191>
 35. Zhang Y, Zhong C, Zhang Q, Chen B, He M and Hu B (2015) Graphene oxide-TiO₂ composite as a novel adsorbent for the preconcentration of heavy metals and rare earth elements in environmental samples followed by on-line inductively coupled plasma optical emission spectrometry detection in *RSC Adv* 5 5996-6005 <https://doi.org/10.1039/C4RA13333A>.
 36. Zhao G, Ren X, Gao X, Tan X, Li J, Chen C, Huang Y, and Wang X (2011) Removal of Pb(II) ions from aqueous solutions on few-layered graphene oxide nanosheets in *Dalton Trans* 40(41) 10945-10952 <https://doi.org/10.1039/C1DT11005E>.